

RADIAL DYNAMICS OF RIGID FRICTION DISKS WITH ALTERNATING STICKING AND SLIDING

Wolfgang Stamm

LuK GmbH & Co. oHG, Bühl
Germany
stammwol@schaeffler.com

Alexander Fidlin

LuK GmbH & Co. oHG, Bühl
Germany
alexander.fidlin@schaeffler.com

Abstract

Many technical systems include rotating friction disks. Assuming pure sticking or sliding in the contact is sometimes not satisfactory to render a precise system dynamics model. Here the plane motions of a simple pin-on-a-disk system and two rigid disks rotating and contacting each other are examined. A numerical study is executed which covers both sticking and sliding states of the frictional contact interface. The static indeterminacy of multiple contacts between rigid bodies during sticking is circumvented by means of an elasto-visco-plastic regularization approach. Sliding is regarded as plastic deformation of an infinitesimal thick layer between the two disks. For higher rotational speeds a limit cycle with intermittent phases of sticking and sliding is observed. Special attention is drawn to the transitions between this limit cycle and a pure sticking solution. The transition is identified as sensitive to the system's parameters and initial conditions.

1 Introduction

Disk clutches [Reik, 1994] and clutch actuation systems [Zink, 2002] are both systems which live on friction. For these systems, friction is not an undesired secondary effect, as it is often the case. In fact their functioning is reliant on the formation of friction. To perform a system dynamics analysis on clutches and their actuators sometimes a precise friction model is needed. As crucial features of such a model one should mention the transitions from sticking to sliding and vice versa as well as contacts distributed along a plane surface.

Dynamics of friction disks have been examined by many researchers. Examples can be found in [Ibrahim, 1994; Mottershead, 2004]. Common applications are dynamics of computer harddisks, friction brakes and a pin-on-disk testing apparatus in tribology (see references in [Ibrahim, 1994; Mottershead, 2004]). The system at hand includes rather uncommon assumptions compared to the work found in literature: Only in-plane motions in radial directions of the two rigid disks (cf. Fig. 1) are considered. The normal pressure is assumed as equally distributed over the contact surface; axial or tilting movement of both disks are ignored. The lower disk in Fig. 1 is driven at constant angular speed and has a rigid support. The upper disk is elastically supported in radial direction, which is interpreted as the elasticity of a shaft. Such a system can be regarded as a strongly simplified clutch model. This interpretation clarifies the focus on radial motions: The frequency of the rotation of clutches and the natural frequency of the disk with elastic support can operate in the same range.

A separate study of this system but with assumed sliding for the numerical simulations is contributed to the conference by the same authors. In this study, for different parameters and initial conditions, the following solutions were found: The driven disk can come to an equilibrium in the vicinity of the rotation centre, which is referred to as self-centering of the disk. Next, a limit cycle solution with large oscillation amplitudes is possible for higher rotational speeds. Under high friction a sticking solution can be found analytically. Finally, due to the coupling between the radial and the

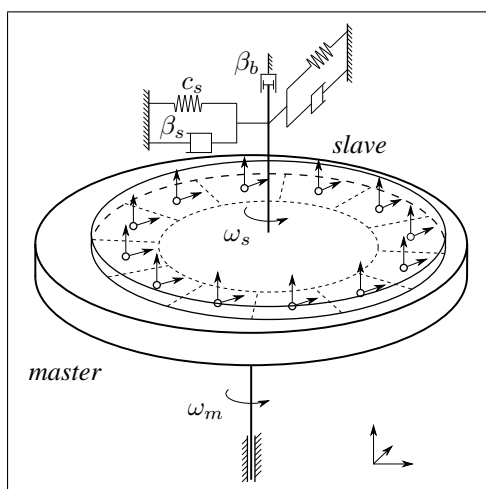


Figure 1. The disk-on-a-disk system with a set of twelve contact points. At each contact point normal and tangential forces are plotted.

rotational motions, this second study reports a destabilization of the limit cycle leading to another one with slowly modulated amplitude. Out of these four basic motions only two are taken into account in the current work: The sticking solution and the limit cycle, which will be shown to exist with alternating sticking and sliding. The contact modeling will allow us to locate the transitions between these two solutions in parameter space.

The friction model proposed hereafter belongs to the class of *penalty* approaches, i.e. relative displacements in contacts during sticking are constrained by means of a penalty force. It is based on an analogy of friction and plasticity, whereat the simplest plasticity model usual in continuum mechanics already suits our needs. The analogy of friction and plasticity has formerly been used in structural mechanics [Laursen, 2002; Michalowski, 1978] and inspired other friction models in robotics and control theory [Canudas, 1995]. Here it is applied in an intuitive and straightforward way to the field of nonlinear rigid body dynamics. There are at least two alternative possibilities to model systems with distributed contacts – classic rigid body mechanics does not belong to them due to the static indeterminacy of multiple contacts during sticking. Firstly, one could consider all involved bodies as elastic and perform a finite element analysis on them. This certainly leads to a high number of degrees of freedom and long computation times which usually conflict with the aims of any dynamics analysis. Secondly, significant progress has been made in *nonsmooth dynamics* [Acary, Brogliato, 2008], where – under some geometric restrictions which can be mostly fulfilled [McNamara, 2006] – it is also possible to represent surface-to-surface contacts between rigid bodies.

2 An Elasto-Visco-Plastic Regularization Model

Consider a regularization of sticking with only spring and damper plus COULOMB friction in the case of sliding. When detecting a transition from sticking to sliding the friction force switches from a position-dependent quantity (spring reaction force) to a velocity-dependent quantity (COULOMB sliding force). In a 2D-contact this would lead to an instantaneous jump of the friction force direction, which is difficult to handle in a numerical integration algorithm. Moreover,

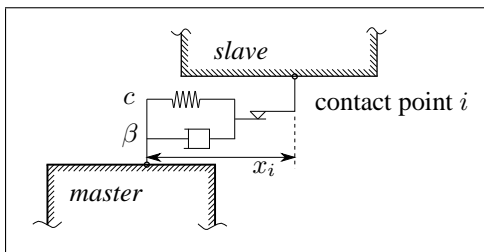


Figure 2. Spring, dashpot and plastic element of the regularization approach

while one can think of colliding micro contacts with discontinuous friction force direction, this shouldn't be the case for contacts on a macroscopic scale. The discretization of the contact surface into a finite set of contact points, which will be done in this regularization approach, should lead to a single contact point representing a sufficiently large number of micro contacts. It is therefore assumed that any discontinuities at micro scale will appear smoothed to an observer on a macro scale.

On these preliminary thoughts the subsequent regularization is based. By means of a plastic element, all contact force directions will change continuously. This might be a very fast process still, depending on the tangential contact stiffness c . In the limit case of $c \rightarrow \infty$ the model degenerates to COULOMB friction.

Suppose we have discretized the two-dimensional frictional contact interface into a set of N contact points as e.g. in Fig. 1. Then for each contact point a regularized friction law is formulated. It is based on the simplest plasticity model suitable for this task, the PRANDTL-REUSS material model or idealized time-independent plasticity [Kachanov, 1971]. The derivation of the friction law will be roughly outlined in the following.

The displacement \mathbf{x}_i of contact point $i, i = 1 \dots N$ during sticking *and* sliding is assumed to consist of elastic (reversible) and plastic contribution:

$$\mathbf{x}_i = \mathbf{z}_i + \mathbf{w}_i, \quad \dot{\mathbf{x}}_i = \dot{\mathbf{z}}_i + \dot{\mathbf{w}}_i \quad (1)$$

Due to the serial connection of the visco-elastic and plastic force elements (cf. Fig. 2) we have:

$$\mathbf{F}_i^f = \mathbf{F}_i^{el} = \mathbf{F}_i^{pl} \quad (2)$$

The force in the elastic element is the reaction force of spring and dashpot:

$$\mathbf{F}_i^{el} = -c\mathbf{z}_i - \beta\dot{\mathbf{z}}_i \quad (3)$$

The plastic deformation is defined as:

$$-\lambda_i \mathbf{F}_i^{pl} = \dot{\mathbf{w}}_i \quad (4)$$

where λ_i controls the occurrence of plastic deformation at each contact point. The multiplier λ_i is introduced in the sense of a 'yield criterion'

$$\lambda_i = \begin{cases} 0 & , \|\mathbf{F}_i^{pl}\| < F_i^{St}(\|\dot{\mathbf{x}}_i\|) \\ \|\dot{\mathbf{w}}_i\| / F_i^{St}(\|\dot{\mathbf{x}}_i\|) & , \|\dot{\mathbf{w}}_i\| > \varepsilon \end{cases} \quad (5)$$

with the scalar-valued function $F_i^{St}(\|\dot{\mathbf{x}}_i\|)$ as a local STRIBECK curve. The two cases of (5) read as follows: We have *sticking* if the regularized friction force

is below its current limit prescribed by the STRIBECK curve and we have *sliding* until the plastic deformation rate (almost) vanishes. The absolute value $\|\dot{\mathbf{w}}_i\|$ is non-negative and any root-finding algorithm will not locate the vanishing plastic deformation rate due to the limits of numerical resolution. Hence, a small threshold ε which defines the onset of sticking is introduced. Inserting (5) in (4) yields:

$$\dot{\mathbf{w}}_i = \begin{cases} \mathbf{0} & , \|\mathbf{F}_i^{pl}\| < F_i^{St}(\|\dot{\mathbf{x}}_i\|) \\ -\|\dot{\mathbf{w}}_i\| \mathbf{F}_i^{pl} / F_i^{St}(\|\dot{\mathbf{x}}_i\|) & , \|\dot{\mathbf{w}}_i\| > \varepsilon \end{cases} \quad (6)$$

which describes the evolution of plastic deformation in the form of an implicit differential equation with discontinuous right hand side. For a plane-to-plane contact \mathbf{w}_i is two-dimensional. Thus for each contact point i we add two degrees of freedom to the system.

Note that plastic deformation *is* sliding within this model. This can be seen from the second case in (6):

$$F_i^{St}(\|\dot{\mathbf{x}}_i\|) \frac{\dot{\mathbf{w}}_i}{\|\dot{\mathbf{w}}_i\|} = -\mathbf{F}_i^{pl} \quad (7)$$

The regularized contact force \mathbf{F}^{pl} opposes the velocity of irreversible relative displacement. Furthermore it is obvious that for low elastic deformation rates¹ we are approximating COULOMB friction:

$$F_i^{St}(\|\dot{\mathbf{x}}_i\|) \frac{\dot{\mathbf{x}}_i}{\|\dot{\mathbf{x}}_i\|} \approx -\mathbf{F}_i^{pl}, \quad \|\dot{\mathbf{z}}_i\| \ll \|\dot{\mathbf{w}}_i\| \quad (8)$$

After some calculus it is possible to obtain from (7) an explicit form of the differential equations for the local plastic deformations:

$$\dot{\mathbf{w}}_i = \begin{cases} \mathbf{0}, & \|\mathbf{F}_i^{pl}\| < F_i^{St}(\|\dot{\mathbf{x}}_i\|) \\ \left(\frac{c}{\beta} (\mathbf{x}_i - \mathbf{w}_i) + \dot{\mathbf{x}}_i \right) \left(1 - \frac{F_i^{St}(\|\dot{\mathbf{x}}_i\|)}{\|c(\mathbf{x}_i - \mathbf{w}_i) + \beta \dot{\mathbf{x}}_i\|} \right), & \left[\|\mathbf{k}_i\| - F_i^{St}(\|\dot{\mathbf{x}}_i\|) \right] / \beta > \varepsilon \end{cases} \quad (9)$$

where the abbreviation

$$\mathbf{k}_i = c(\mathbf{x}_i - \mathbf{w}_i) + \beta \dot{\mathbf{x}}_i \quad (10)$$

is used. Note that the quantities \mathbf{x}_i and $\dot{\mathbf{x}}_i$ are available at all contact points as kinematic transforms of the system's rigid bodies degrees of freedom. The coupling between the rigid body and friction subsystems is then completed by the frictional forces (3) which act at the contacting bodies. Thus the equations of motions are augmented by a set of $2N$ equations for the internal friction variables.

¹which we would have to call *gross sliding* to concur with other friction models

3 Numerical Solutions

An event-based ROSENBROCK integration scheme has been used to solve the coupled system of rigid body motions and friction states. The algebraic constraints were introduced as LANGRANGIAN multipliers in the well-known form of BAUMGARTE [Baumgarte, 1976]. Much attention has to be paid to the event detection algorithm and computational efficiency, because the systems examined here can feature a high number of stick-slip transitions (the number of observed transitions occasionally exceeded 100.000 within the desired simulation time). However, the challenging numerics of such systems is not spotlighted here in order to maintain the focus of this paper.

In the following subsections the results of a high number of simulation runs on a pin-on-a-disk system and a disk-on-a-disk system are presented. They complement the mentioned separate study with the assumption of pure sliding in the contact, which is also contributed to this conference. From this study it is known that both systems reveal a limit cycle with large oscillation amplitudes for higher angular speeds. It is also known that for higher frictional forces a sticking solution exists.

All system parameters have been chosen arbitrarily, often close to their SI-unit. It is possible to identify the same phenomena for a set of more realistic parameters, as the topology of the solution space is unaffected by the parameters' absolute values.

3.1 Pin-On-a-Disk System With Single Contact

As a first simplification the driven disk (*slave* in Fig. 1) is replaced by a pin with a single contact point at its tip (cf. Fig. 3). The driving disk (*master*) with rigid support is driven at constant angular speed $\omega_m = 1.1$ rad/s. The two springs and dampers confining the pin's motion in radial direction have a linear stiffness of $c_s = 1$ N/m and a damping coefficient of $\beta_s = 0.1$ Ns/m. The mass of the pin is set to $m_s = 1$ kg. A total normal force of $F^n = 1$ N acts in the frictional contact interface. The tangential contact stiffness² has been set to $c = 253$ N/mm.

Figure 4 depicts a typical trajectory of a solution with outer limit cycle. Starting from the offset position $x_{m,s} = 0.1$ m with the elastic support of the pin at rest, the pin follows the counterclockwise rotation of the master disk with an increasing radius. In the lower left segment of Fig. 4 we encounter a sticking regime. Here the pin moves on a circular orbit prescribed by the master disk. In the upper and right segment of Fig. 4 we find a sliding regime. Instead of a circular orbit the distance between pin and rotation axis first increases and then decreases again. In case of the limit cycle this is shown in Figure 5. The amplitude of this deviation from the circle a can be used to describe the shape of the limit cycle. In Figure 6 the dependency of the limit cycle shape on the frictional coefficient is shown. We

²the regularized contact parameters were selected according to rules omitted here; basic ideas can be found in [Vielsack, 1996]

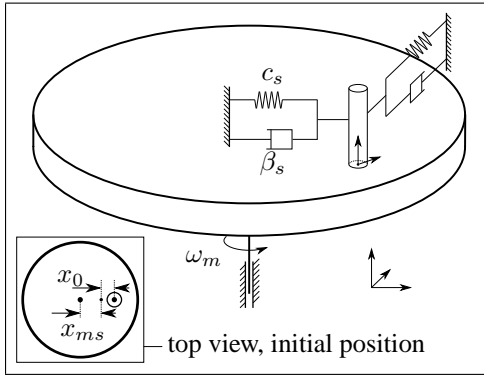


Figure 3. The pin-on-a-disk system with a single contact point. The small top view detail displays the offset between master disk and slave pin x_{ms} at spring rest position and the initial spring deflection x_0 .

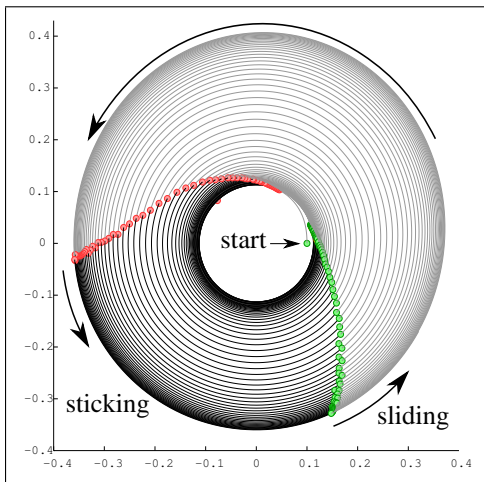


Figure 4. Typical trajectory of driven pin or disk leading to a limit cycle with sticking (dark) and sliding (light) segments

observe a linear relationship between μ and the shape measure a . However, an obvious reason for the linear character of this relationship cannot be given.

Alongside with the described solution with alternating phases of sticking and sliding a solution characterized by permanent sticking exists. This solution can be reached starting from the first one by just increasing the frictional coefficient μ . After a short phase of sliding created by the initial condition the pin remains sticking on a circular orbit with the radius of the first (innermost) sticking segment in Fig. 4. The transition from limit cycle to sticking solution manifests itself in a jump of the pin's stationary oscillation amplitude. This jump happens in a small range of μ and is characterized by a topological change of the solution, hence it is a bifurcation.

The location of the bifurcation is identified numerically by subsequent simulation runs. For each run the simulation time is adjusted until the outer limit cycle is reached or the low amplitudes of the sticking solution remain constant. Then iteratively the frictional coefficients μ are modified until the jump be-

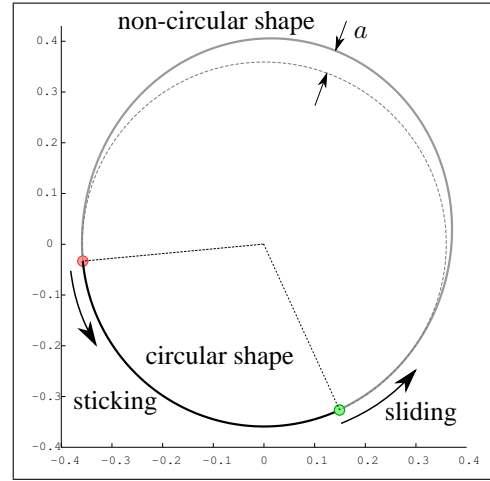


Figure 5. Limit cycle trajectory, circular shape during sticking and non-circular during sliding

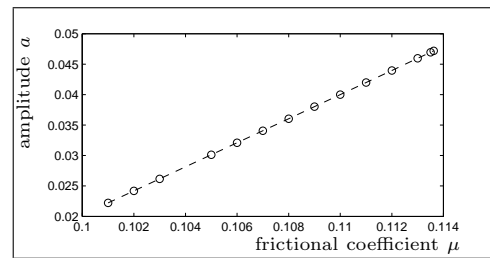


Figure 6. Deviation from circle a during sliding for different friction coefficients μ

tween limit cycle and sticking solution is found in an interval $\Delta\mu = 10^{-4}$.

In Figure 7 one can see the dependency of the bifurcation on the axes misalignment x_{ms} . As an additional information the middle plot with $x_{ms} = 0.1$ m shows the results of the single simulation runs as dots; it is visible how the location of the jump has been iterated. The size of the limit cycle which is plotted in Fig. 7 has

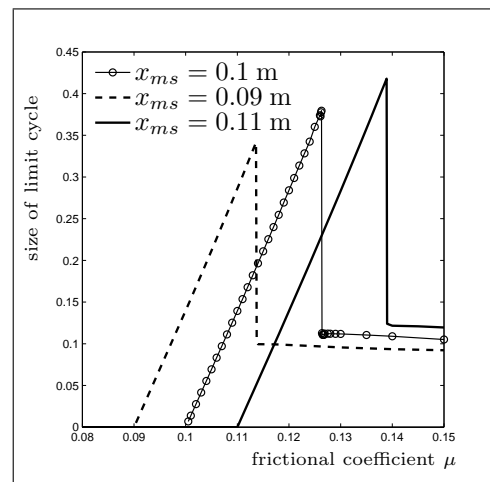


Figure 7. Transitions from limit cycle to sticking solution for different offsets

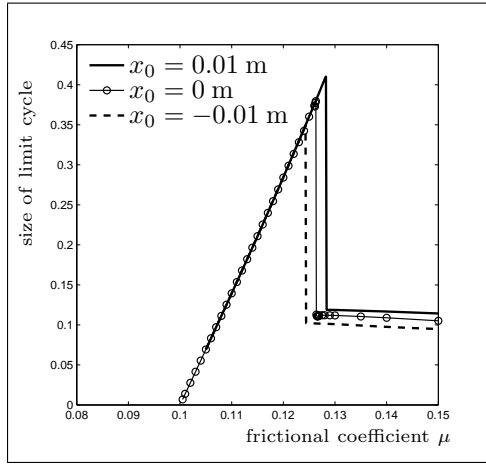


Figure 8. Transitions from limit cycle to sticking solution for different initial conditions

been measured the following way: For solutions with high amplitudes the radius of the sticking segment on the limit cycle (lower left in Fig. 5) and for the solutions with low amplitudes the radius of the full (sticking) circle has been employed as ‘size’. Note that for different values of x_{ms} you get also different limit cycles.

A slightly different behavior is obtained when the axes misalignment x_{ms} is kept constant but instead the initial displacement x_0 of the pin is modified. As depicted in Figure 8, again the bifurcation can be shifted to the left or right. The domain of attraction of the limit cycle solution in phase space can be interesting for technical applications: The exact initial state of e.g. a clutch system is usually unknown. Therefore, even when the parameters of the system are well identified, the occurrence of the large limit cycle can only be precluded by estimation of the initial state and comparing it to the domain of attraction of this type of solution.

3.2 Two Friction Disks

In the last section, the single contact point at the pin’s tip did not transmit a friction torque. Now, by replacement of the pin with the *slave* disk, this friction torque is transmitted and therefore an additional degree of freedom is introduced: the rotation of the *slave* body around its central axis. With the viscous damping β_b a braking torque can be generated. Of course, by increasing β_b one can obtain permanent slip between the two disks. Here β_b was kept small in order to allow sticking and to examine the transitions from the limit cycle solution to the sticking solution as with the previous system.

Firstly, β_b was set to zero and the moment of inertia of *slave* was given a comparably small value of $J_s = 0.02 \text{ kg m}^2$, so it can rotate easily. All other parameters were copied from the pin-on-disk system. As one would expect, the pin-on-disk and the disk-on-disk system behave almost identical now. Figure 7 is not repeated here, instead only the location of the jump

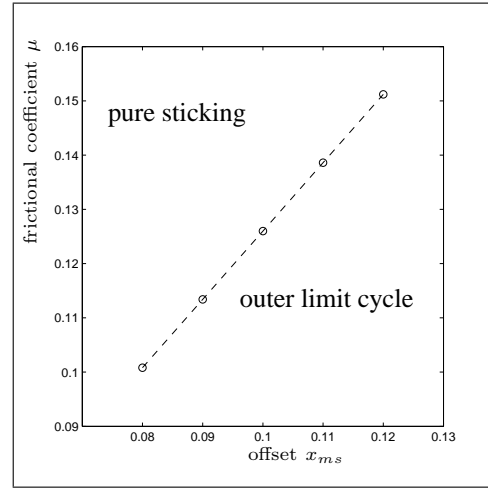


Figure 9. Bifurcation plot with axes offset and frictional coefficient as bifurcation parameters

is plotted in the (x_{ms}, μ) -parameter plane. The result is given in Figure 9. For each of the points in the bifurcation diagram many numerical simulations have to be run in order to locate the jump with a precision of $\Delta\mu = 10^{-4}$. Therefore only five data points are given in the diagram. Perhaps the obtained linear relationship is not surprising, as the centripetal acceleration ($a = \omega^2 r$) depends linearly on the offset $r = x_{ms}$.

The two regions *pure sticking* and *outer limit cycle* adjacent to the line in Figure 7 can be seen as follows: for a given μ one can either ‘stabilize’ the system by decreasing x_{ms} and herewith enforce a sticking solution or ‘destabilize’ the system by increasing x_{ms} .

Analogous to the pin-on-disk system the initial condition x_0 was chosen as another bifurcation parameter (the remaining initial conditions $y_0 = \dot{x}_0 = \dot{y}_0 = 0$ kept natural). Again Fig. 8 is not repeated for the disk-on-disk system, instead only the bifurcation in the (x_0, μ) -plane is plotted in Figure 10, a two-dimensional cross section of the domain of attraction of the large limit cycle solution in a multidimensional parameter and phase space of the system. For a constant value of μ we can ‘stabilize’ the system with the sticking solution by placing the elastic supported body *slave* initially closer to the rotation centre of *master*. We can ‘destabilize’ the system by initial placement of *slave* in a distant position from the rotation centre.

As a last result, the brake coefficient β_b was taken as a bifurcation parameter. The corresponding bifurcation diagram in the (β_b, μ) -parameter plane is presented in Figure 11. It can be seen clearly, that for a given frictional coefficient μ one can migrate from a sticking solution with low amplitudes to a sticking/sliding limit cycle solution with high amplitudes by increasing the brake load. Recall that for the assumption of pure sliding in the contact interface a similar limit cycle with high amplitudes is obtained. Therefore it is not surprising to arrive at the limit cycle as we enforce more slip by increased brake torque.

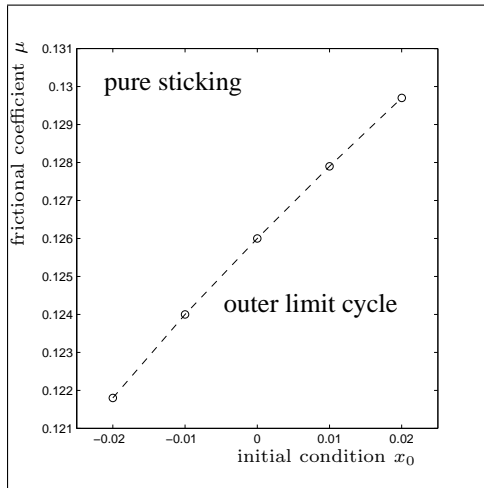


Figure 10. Bifurcation plot with initial condition and frictional coefficient as bifurcation parameters

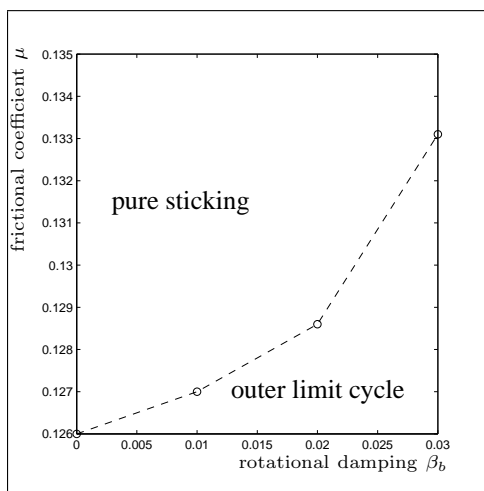


Figure 11. Bifurcation plot with rotational damping and frictional coefficient as bifurcation parameters

4 Conclusions

The reported regularization approach is based on the analogy of friction and plasticity, applied to rigid body dynamics. It is used here for both a single contact situation and multiple contacts distributed along a two-dimensional surface³. Desirable features of any friction model such as local STRIBECK curves or reversible, *true stiction* are represented. Despite the event-based integration scheme, where computational resources have to be spent on the location of discontinuities, the contact modeling is suitable for simulating radial dynamics of friction disks.

With the friction model it is possible to perform a numerical parameter study and locate bifurcations in the systems' parameter and phase spaces. The dependency of the sudden jump from one solution to another on a couple of control parameters has been demonstrated.

The results obtained here encourage us to apply the contact model to a real-world system in the future, e.g. a disk clutch.

Radial dynamics of the disk-on-disk system and the pin-on-disk system are similar in terms of limit cycle to sticking transition. In both cases the bifurcation can be shifted qualitatively the same way by the selected control parameters. Significant differences between the two sample systems occur when either a brake torque is applied at the driven disk or – not reported in the results section but similar to the effect of the brake torque – the moment of inertia J_s of *slave* is increased.

References

- Baumgarte J. (1976) *Celestial Mechanics* 13:247
- Canudas de Wit C. (1995) *IEEE Transactions on Automatic Control* 40:419-425
- Acary V. and Brogliato B. (2008) *Numerical Methods for Nonsmooth Dynamical Systems*, Springer, Berlin Heidelberg New York
- Ibrahim R. A. (1994) *Applied Mechanics Reviews* 47:209-226
- Kachanov L. M. (1971) *Foundations of the Theory of Plasticity*, North-Holland
- Laursen T. A. (2002) *Computational Contact and Impact Mechanics*, Springer, Berlin Heidelberg New York
- Michalowski R., Mróz Z. (1978) *Archives of Mechanics*, 30:259-276
- McNamara S. (2006) *Proceedings of the IUTAM Symposium on Multiscale Problems in Multibody System Contacts*, Stuttgart
- Ouyang H. and Mottershead J. E. (2004) *ASME Journal of Applied Mechanics* 71:753-758
- Reik W. (1994) *5th LuK Symposium*, 43-63
- Vielsack P. (1996) *ZAMM* 76:439-446
- Zink M., Shead R. and Welter R. (2002) *7th LuK Symposium*, 35-47

³for the single contact point the penalty approach is not crucial. One could calculate the friction force during sticking from a static equilibrium.